



# Mixed Curved Finite Strip Analysis of Cylindrical Shells Using B3-Spline Function

Salah Barony<sup>1</sup>, Ezzedin Galuta<sup>2</sup>, Wedad Al-Salah<sup>3</sup>

<sup>1</sup>Civil Engineering Department, Libyan Academy of Graduate Studies, Tripoli, Libya)

<sup>2</sup>Civil Engineering Department, University of Tripoli, Tripoli, Libya

<sup>3</sup>Civil Engineering Department, University of Garyan, Garyan, Libya

## ABSTRACT

*This paper presents the development of the mixed formulation of curved finite strip element for cylindrical shells using the cubic B3 spline function. The curved shell element is divided into a number of longitudinal curved strips. Each strip element has two nodal lines with four knot amended splines in addition to the existing of interference between the first and last ends amended splines in the whole three elementals. The nodal degrees of freedom are consisted of three displacements (i.e.  $u$ ,  $v$ , and  $w$ ) and three moments (i.e.  $M_x$ ,  $M_y$  and  $M_{xy}$ ) in  $x$ ,  $y$  and  $z$  directions respectively. The validity of the mixed formulation is tested through two numerical examples of cylindrical shell roofs. The important design quantities such as vertical deflection and lateral moments are found to be in good agreement, when compared with an accurate solution.*

**Keywords:** *Mixed formulation, curved finite strip, B3-spline function and cylindrical shells.*

## I. INTRODUCTION

The Finite Strip (FS) method was based on harmonic functions and proved to be an efficient tool for analyzing structures with constant geometrical properties along the longitudinal direction. The Spline Finite Strip (SFS) method was developed from the semi-analytical (FS) method originally derived by Cheung [1]. The (SFS) method has enhanced the finite strip method to overcome the difficulties arising in the classical finite strip method by allowing more complex geometry and different types of loading to be modelled based on splines. The (SFS) method has been fully developed for the elastic structural analysis of folded plate structures [2]. Subsequently, the isoparametric concept was applied to the spline finite strip method by Au and Cheung for the linear in-plane stress and bending analyses of Mindlin plates [3] and degenerated shells [4]. This extension allowed structures having a distorted longitudinal axis to be efficiently analyzed with the finite strip method.

The mixed formulation is obtained using variational principles that can be regarded as extension of the principle of stationarity of total potential energy. This principle uses the primary and secondary variables in the conventional formulation as dependent variables and thus its objective is to determine the secondary variables with the same order of accuracy directly rather than from post computations. Abdunnaser [5] introduced the mixed finite strip formulation and presented a comparative study between mixed and stiffness formulation for plate problems. Barony, et al [6] presented a mixed formulation of a two-nodal line curved finite strip element to analyze curved cylindrical shells with simply supported edges.

In this paper, an efficient formulation of mixed finite strip using cubic spline function to analyze cylindrical shell problems is presented. In the mixed formulation, moments are included as primary variables in addition to

displacement components. Two numerical examples of shell roofs with different boundary conditions are presented to illustrate the accuracy of the method.

## II. MIXED SPLINE FINITE STRIP FORMULATION

The mixed formulation of curved finite strip element for cylindrical shells using the cubic B3 spline function is presented in the following sections. The formulation is obtained by using variational principles that can be regarded as extension of the principle of stationarity of total energy.

### 2.1 B3-Spline Function

The B3cubic spline of unit length is defined as:

$$\phi_{j,3}(y) = \frac{1}{6} \begin{cases} 0 & | y < y_{j-2} \\ (y - y_{j-2})^3 & | y_{j-1} \leq y < y_{j-2} \\ 1 + 3(y - y_{j-1}) + 3(y - y_{j-1})^2 - 3(y - y_{j-1})^3 & | y_{j-1} \leq y < y_j \\ 1 + 3(y_{j+1} - y) + 3(y_{j+1} - y)^2 - 3(y_{j+1} - y)^3 & | y_j \leq y < y_{j+1} \\ (y_{j+2} - y)^3 & | y_{j+1} \leq y < y_{j+2} \\ 0 & | y > y_{j+2} \end{cases} \quad (1)$$

In (1),  $\phi_j(y)$  represents the  $j^{th}$  component of the cubic spline series, having non-zero values only over four consecutive sections centered over the  $j^{th}$  node, while  $y$  is the natural longitudinal coordinate. Figure 1 shows the shape of a single B3 spline function while Fig. 2 shows a series of spline functions of equal magnitude.

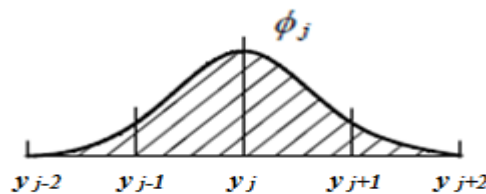


Fig. 1:  $j^{th}$  component of the B3-Spline

By inspection of (1) and Fig. 1, it follows that the generic  $j^{th}$  spline component is defined over four consecutive sections and centered on the  $j^{th}$  node. A full B3-Spline series comprises  $m+3$  components, i.e.  $m+3$  nodes per nodal line, as shown in Figure 2, where with "m" we denote the number of sections subdividing the strip and, consequently, each nodal line. It also follows that the coordinate  $y$  spans from zero to  $m$  between the two ends.

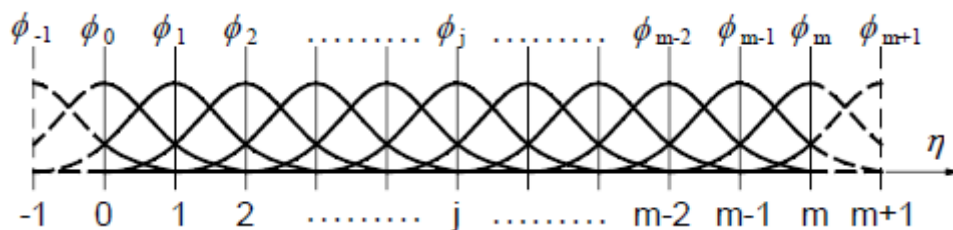


Fig. 2: Complete B3-Spline series.

In order to interpolate any arbitrary function  $S(y)$  along a line at an interval  $[a, b]$  in  $y$  direction by using spline technique, the interval should be divided into a number of segments (or elementals). The arbitrary function  $S(y)$  can be expressed as:

$$s(y) = \sum_{i=-1}^{m+1} \alpha_i \phi_i(y) \tag{2}$$

Where,  $m$  is the number of equal segments into which the domain is discretized,  $\phi_i$  is a local B3-spline spanning over four consecutive segments and  $\alpha_i$  is the coefficient of  $\phi_i$ .

### 2.2 Strip Geometry

The curved shell is discretized into a set of longitudinal strip elements and each strip element consists of two nodal lines as shown in Fig. 3. The nodal degrees of freedom on each nodal line are consisted of three displacements (i.e.  $u, v,$  and  $w$ ) and three moments (i.e.  $M_x, M_y,$  and  $M_{xy}$ ) in  $x, y$  and  $z$  directions respectively. The actual geometry at each nodal circle is used to evaluate the constants of the fifth order polynomial assigned for the substitute curve, which is represented by the non-dimensional local co-ordinates of the element ( $\eta, \zeta$ ). The fifth order polynomial is given by (3) while the local co-ordinates of the curved element are shown in Fig. 4.

$$\eta = a_0 + a_1\zeta + a_2\zeta^2 + a_3\zeta^3 + a_4\zeta^4 + a_5\zeta^5 \tag{3}$$

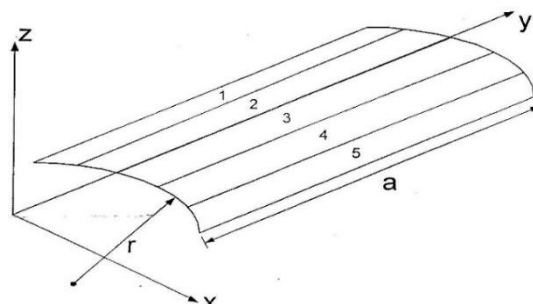


Fig. 3: Discretized shell into a set of longitudinal elements

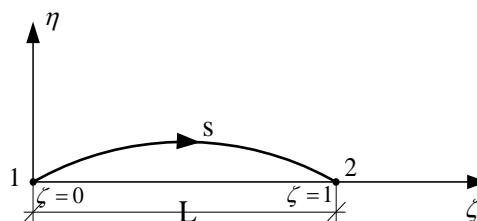


Fig. 4: Local normalized coordinates of the curved element

### 2.3 Evaluation of Nodal Variables

The nodal line variables in matrix notation can be written as:

$$m^T = (M_{x1} \quad M_{y1} \quad M_{xy1} \quad M_{x2} \quad M_{y2} \quad M_{xy2})$$



$$\begin{aligned}
 u^T &= (u_{x1} \quad v_{y1} \quad w_{z1} \quad u_{x2} \quad v_{y2} \quad w_{z2}) \\
 q^T &= (q_{x1} \quad q_{y1} \quad q_{z1} \quad q_{x2} \quad q_{y2} \quad q_{z2})
 \end{aligned}
 \tag{4}$$

Where  $m$ ,  $u$  and  $q$  represent the nodal moment, displacement and service load matrices respectively. The subscripts one and two refer to the nodal lines  $i$  and  $j$ . Also (4) can be written as:

$$\begin{aligned}
 m &= G M \\
 u &= J U \\
 q &= P Q
 \end{aligned}
 \tag{5}$$

where

$$J = G = P = \begin{bmatrix} a_1 & 0 & 0 & a_2 & 0 & 0 \\ 0 & a_1 & 0 & 0 & a_2 & 0 \\ 0 & 0 & a_1 & 0 & 0 & a_2 \end{bmatrix}, \quad a_1 = 1 - \frac{s}{l} \quad \text{and} \quad a_2 = \frac{s}{l}
 \tag{6}$$

Where "s" is the arc length coordinate of the strip and "l" is the strip arc length. Therefore, the nodal unknowns of the finite strip can be arranged in the form:

$$\delta_s^T = \left[ u_{x1} \quad v_{y1} \quad w_{z1} \quad M_{x1} \quad M_{y1} \quad M_{xy1} \quad u_{x2} \quad v_{y2} \quad w_{z2} \quad M_{x2} \quad M_{y2} \quad M_{xy2} \right]
 \tag{7}$$

### 2.4 Variational Principle

The functional used by Barony and Tottenham [7] for the shells of revolution which was applied to linear analysis of axisymmetric shells of revolution is given by (8) as:

$$\pi = \int_0^a \int_{s_0}^{s_1} (\omega_{ue} - \omega_{\sigma m} - \omega_{\sigma s} + \omega_{\gamma s} + \omega_u) ds dy + \psi \Big|_{s_0}^{s_1} \Big|_0^a
 \tag{8}$$

Where

$\omega_{ue}$ : is the strain energy of the in-plane stresses.

$\omega_{\sigma m}$ : is the complementary energy of the stress couples.

$\omega_{\sigma s}$ : is the complementary energy of the transverse shear strains.

$\omega_{\gamma s}$ : is the work done by the transverse shear.

$\omega_u$ : is the work done by the applied loads.

$\psi$ :  $\psi(\delta, M)$  is a function of the variables  $\delta$  and  $M$  giving the work done at the boundaries where  $\delta$  and/or  $M$  are specified.

In this formulation the free and independent variables are displacements ( $\delta$ ) and moments ( $M$ ), i.e.



$$\pi(\delta, M) = \pi(u, v, w, M_x, M_y \text{ and } M_{xy})$$

Substituting the energies in the integrand of (8) and the nodal values u and m of (4) into (6), and using linear expansions in terms of the meridional curve, (8) develops into:

$$\begin{aligned} \pi(\delta, M) = \pi(u, m) = & \frac{1}{2} u^T \left\{ \int_0^a \int_{s_0}^{s_1} (F^T k_n F) ds dy \right\} u \\ & - \frac{1}{2} m^T \left\{ \int_0^a \int_{s_0}^{s_1} (N^T f_x N) ds dy \right\} m \\ & - \frac{1}{2} m^T \left\{ \int_0^a \int_{s_0}^{s_1} (H^T f_y H) ds dy \right\} m \\ & + m^T \left\{ \int_0^a \int_{s_0}^{s_1} (H^T I) ds dy \right\} u \\ & - q^T \left\{ \int_0^a \int_{s_0}^{s_1} (N^T N) ds dy \right\} u + \psi y \Big|_{s_0}^a \Big|_0^a \end{aligned} \quad (9)$$

The parameters matrices inside each integrand in (9) are dependent only on the geometrical and elastic properties of each element, therefore, (9) can be written in a more concise form as:

$$\begin{aligned} \pi = & \frac{1}{2} u^T k_m u - \frac{1}{2} m^T k_b m - \frac{1}{2} m^T k_s m \\ & + m^T k_c u - q^T k_p u + A \Big|_0^a + B \Big|_0^a \end{aligned} \quad (10)$$

Where

$$\begin{aligned} k_m = & \int_0^a \int_0^l (F_m^T k_n F_m) ds dy \\ k_b = & \int_0^a \int_0^l (N_m^T f_x N_m) ds dy \\ k_s = & \int_0^a \int_0^l (H_m^T f_y H_m) ds dy \\ k_c = & \int_0^a \int_0^l (H_m^T I_m) ds dy \\ k_p = & \int_0^a \int_0^l (N_m^T N_m) ds dy \end{aligned} \quad (11)$$

Details of the matrices  $F_m$ ,  $H_m$ ,  $N_m$  and  $I_m$  in (11) can be found in Ref. [8]. To minimize the functional, as it appears in (10), a first variation is considered, with respect to the two systems of nodal values u and m, which produces a set of linear equations which can be solved for the nodal unknowns ( $\delta$ ).

$$\frac{\partial \pi}{\partial u} = k_m u - k_c^T m - k_p^T q = 0 \quad (12)$$

$$\frac{\partial \pi}{\partial m} = -k_b m - k_s m + k_c u = 0 \quad (13)$$

Equations 12 and 13 can be written in a matrix form as:



$$k \delta = F$$

Details of the assembling of the  $k$  matrix, the displacement  $\delta$  and load  $F$  vectors of (14) are presented in Ref. [9]. The "k" matrices in (11) can be evaluated numerically. For example, for curved strip of length "l" along x- axis and width "a" along y-axis and the coordinates of its nodal lines are 1 (0, y) and 2 (L, y), the matrix  $k_m$  in (11) can be written in the form:

$$k_m = \int_0^a \int_0^l (\theta^T \cdot J^T \cdot [\phi_m]^T) \cdot \partial_1^T \cdot k_n([\phi_m] \cdot J \cdot \theta) \cdot ds dy \quad (15)$$

The term " $k_m u$ " in the first part of (10), a system of simultaneous equations can be written in matrix form as:

$$k_m u = \begin{bmatrix} [k_{m11}] & [k_{m12}] & [k_{m13}] & [k_{m14}] & [k_{m15}] & [k_{m16}] \\ [k_{m21}] & [k_{m22}] & [k_{m23}] & [k_{m24}] & [k_{m25}] & [k_{m26}] \\ [k_{m31}] & [k_{m32}] & [k_{m33}] & [k_{m34}] & [k_{m35}] & [k_{m36}] \\ [k_{m41}] & [k_{m42}] & [k_{m43}] & [k_{m44}] & [k_{m45}] & [k_{m46}] \\ [k_{m51}] & [k_{m52}] & [k_{m53}] & [k_{m54}] & [k_{m55}] & [k_{m56}] \\ [k_{m61}] & [k_{m62}] & [k_{m63}] & [k_{m64}] & [k_{m65}] & [k_{m66}] \end{bmatrix} \begin{bmatrix} [u_1] \\ [v_1] \\ [w_1] \\ [u_2] \\ [v_2] \\ [w_2] \end{bmatrix} = \begin{bmatrix} [F_{x1}] \\ [F_{y1}] \\ [F_{z1}] \\ [F_{x2}] \\ [F_{y2}] \\ [F_{z2}] \end{bmatrix} \quad (16)$$

Each submatrix, i.e.  $k_{m11}$  can be computed as follows:

$$[k_{m11}] = \frac{Eh}{(1-\nu^2)} \int_0^a \int_0^l \left( \frac{c_1^2}{l^2} [\phi_u]^T [\phi_u] + C \cdot \frac{s_1 c_1}{l} \cdot a_1 \cdot [\phi_w]^T [\phi_u] + C \cdot a_1 \cdot \frac{s_1 c_1}{l} [\phi_u]^T [\phi_u] + \left( \frac{1-\nu}{2} \right) \cdot a_1^2 \cdot c_1^2 [\phi_u]^T [\phi_u] + C^2 \cdot a_1^2 \cdot s_1^2 [\phi_w]^T [\phi_w] \right) ds \cdot dy$$

Equation (17) is evaluated numerically using a computer program. Details of all parameters and functions associated with "k" matrices as well as the solution of the linear system of equations are defined in Ref. [9].

### III. RESULTS AND DISCUSSION

The validity of the mixed formulation of Curved Finite Strip element using B3 splines function (CFS-B3) and the accuracy of results are demonstrated by two numerical examples of cylindrical shells roofs using different boundary conditions. In example 1, the cylindrical shell is simply supported along the curved and straight edges (longitudinal and transverse directions) and it is subjected to a loading of  $q = 90 \text{ lb/ft}^2$ . The thickness of the shell is 3 inches and the radius of curvature is 25 feet while the length of the straight edge is 50 feet. Details of the shell geometry and material properties of example 1 are given in Fig. 5. The results obtained from the (CFS-B3) were compared with the Shallow Shell Theory (SST) solution presented by Scordelis [10].

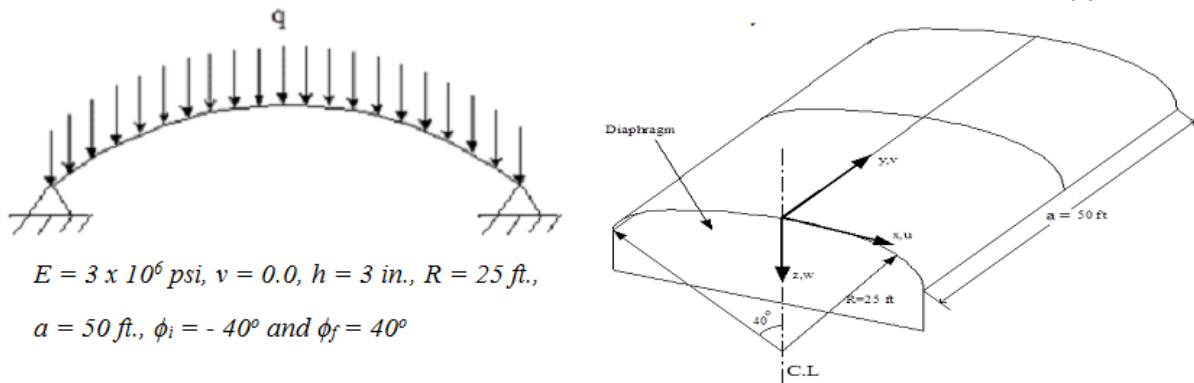


Fig.5: Details of the shell geometry and material properties for example 1.

The convergence of the results is tested by changing the number of the longitudinal strip elements (NE). Two different meshes with eight and ten longitudinal strip elements were used in the test. Due to symmetry, only the results of the half shell are presented. (i.e.  $\phi$  varies from  $0^\circ$  to  $40^\circ$ ). The results of the vertical displacement ( $w$ ) and the transverse moment ( $M_x$ ) along the center of the shell ( $a = 25$  ft.) for example (1) obtained by (CFS-B3) are compared with the (SST) solution and summarized in Tables 1, and 2. The difference in results between (CFS-B3) and (SST) solutions are demonstrated by (%) under (CFS-B3) results in all the Tables.

Table 1: Vertical displacement and transverse moment (NE = 8).

$\phi$	Vertical Displacement, $w \times 10^{-2}$ (in)		Transverse Moment $M_x \times 10^{-5}$ (Ib.ft/ft)	
	SST	CFS-B3 (%)	SST	CFS-B3 (%)
$40^\circ$	0	0	0	0
$30^\circ$	- 1.479	- 1.500 (1.4%)	2.265	2.760 (21%)
$20^\circ$	- 0.0193	- 0.0195 (1.0%)	1.330	1.420 (6.7%)
$10^\circ$	3.121	3.220 (3.2%)	-0.0257	-0.0261 (1.5%)
$0^\circ$	4.672	4.780 (2.3%)	-0.599	-0.599 (0%)



Table 2: Vertical displacement and transverse moment (NE = 10).

$\phi$	Vertical Displacement, $w \times 10^{-2}(\text{in})$		Transverse Moment $M_x \times 10^{-5}(\text{lb.ft/ft})$	
	SST	CFS-B3 (%)	SST	CFS-B3 (%)
40°	0	0	0	0
32°	-1.221	-1.233 (1.0%)	2.020	2.050 (0.7%)
24°	-1.144	-1.137 (0.6%)	1.980	2.0 (1.0%)
16°	1.554	1.486 (4.3%)	0.599	0.597 (0.3%)
8°	3.121	3.255 (4.3%)	-0.0257	-0.0261 (1.5%)
0°	4.672	4.780 (2.3%)	-0.599	-0.599 (0%)

It can be observed from the results in Tables 1 and 2, the vertical displacements obtained by (CFS-B3) are in a good agreement with those calculated by (SST) solution. A little improvement is observed when the number of strip elements is increased, i.e. the maximum difference in the results of vertical displacements is 4.3% when 10 strip elements is used.

In general, the results of the transverse moment using (CFS-B3) converge as the number of strip elements is increased and better results were obtained in strip elements near the center of the shell. In Table 1, when eight strip elements (i.e. NE = 8) are used, the value of the transverse moment is 21% higher than the (SST) solution at the strip near the simply supported edge (i.e.  $\phi = 30^\circ$ ), whereas the maximum difference in the results of the transverse moment is reduced to 1.5% when ten strip elements are used. It can be concluded from Tables 1 and 2, that the transverse moment results for all meshes improved in strips that are away from the supported edge.

In example 2, the same cylindrical shell of the previous example is solved using (CFS-B3) but with different boundary conditions. The shell straight edges are free, while the curved edges are supported on rigid diaphragms along their plan. The same loading and material properties given previously in Figure 5 were used for example 2. The results obtained from the (CFS-B3) were compared with the (SST) solution in Tables 3 and 4.

Table 3: Vertical displacement and transverse moment (NE = 8).

$\phi$	Vertical Displacement, $w$ (in)		Transverse Moment $M_x \times 10^{-5}(\text{lb.ft/ft})$	
	SST	CFS-B3 (%)	SST	CFS-B3 (%)
40	3.703	3.811 (0.8%)	0	0
30	2.364	2.385 (0.8%)	2.53	2.47 (2.3%)
20	0.952	0.953 (0.1%)	16.70	14.3 (14.3%)
10	0.140	0.140 (0%)	27.90	29.8 (6.8%)
0	-0.548	-0.564 (2.9%)	31.60	30.40 (3.7%)

Table 4: Vertical displacement and transverse moment (NE = 10).



$\phi$	Vertical Displacement, w (in)		Transverse Moment, $M_x \times 10^{-5}$ (Ib.ft/ft.)	
	SST	CFS-B3 (%)	SST	CFS-B3 (%)
40	3.703	3.703 (0.%)	0	0
32	2.642	2.640 (0.1%)	0.38	0.39 (2.6%)
24	1.499	1.499 (0.%)	10.60	10.90 (2.8%)
16	0.452	0.452 (0.%)	21.70	21.90 (0.9%)
8	-0.284	-0.284 (0.%)	28.90	30.0 (3.8%)
0	-0.548	-0.546 (0.3%)	31.20	30.40 (2.5%)

In Tables 3 and 4, excellent agreement is shown between the results of the vertical displacements obtained by (CFS-B3) and those obtained from (SST) solution. Furthermore, when the 10 strip elements were used, i.e. N = 10, the (CFS-B3) gives almost identical results to the SST solution. Similar observation can be made for the results of the transverse moments when the number of the longitudinal strip elements are increased. The lateral moments converge quickly when more strip elements (i.e. NE = 10) are used. The corresponding maximum difference in the results of the transverse moment is reduced to 3.8%.

For comparison purpose, the variations of the vertical displacements and transverse moments along the curved shell at the mid of free edges for SST and CFS-B3 solutions using both meshes are shown in Figures. 6 and 7.

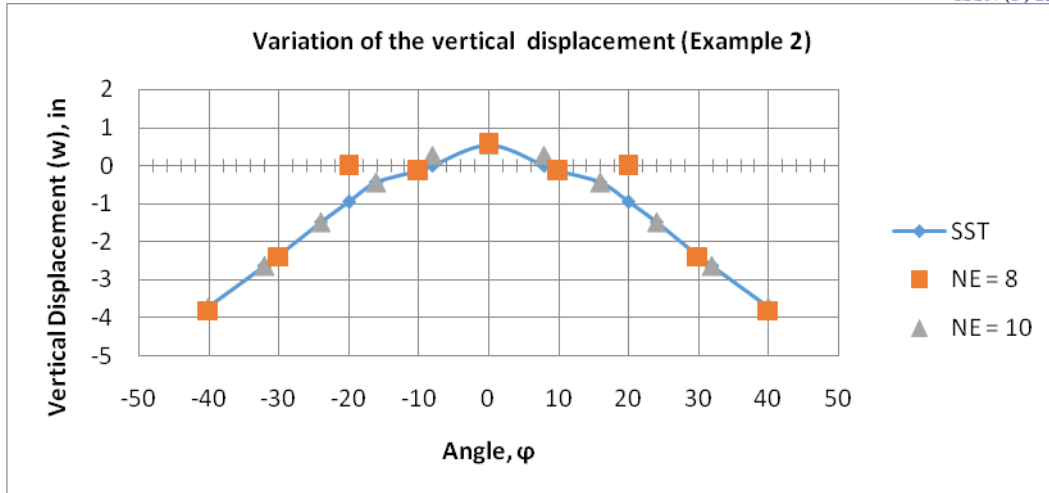


Fig. 6: Variation of the vertical displacement for example 2.

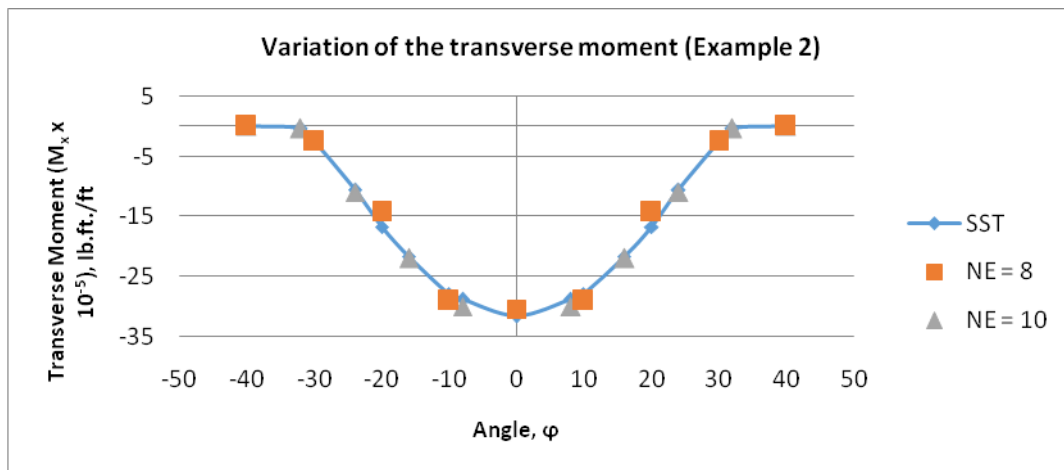


Fig. 7: Variation of the transverse moment for example 2.

#### IV. CONCLUSION

The formulation and application of the mixed curved finite strip using B3-spline function to analyze cylindrical shells have been presented. The numerical examples have demonstrated the accuracy of the mixed formulation in dealing with curved shell problems. The accuracy of the results has been compared with the Shallow Shell Theory solution. The comparison of the results has shown that a good agreement of displacements and moments can be obtained with the mixed formulation using a relatively small number of strip elements.

#### REFERENCES

- [1] Cheung, YK. Finite strip method in structural analysis. Oxford; New York: Pergamon Press, 1976.
- [2] Fan, SC, Spline finite strip in structural analysis., Thesis, University of Hong Kong, 1982.
- [3] Au, FTK, Cheung, YK. Isoparametric spline finite strip for plane structures, Computers & Structures 1993; 48(1):23-32.
- [4] Cheung, YK, Au, FTK. Isoparametric spline finite strip for degenerate shells. Thin-Walled Structures 1995;21(1):65-92.



- [5] Abdunnaser M. Younes, Finite Strip Method – A comparative study between the stiffness and the mixed approaches, M.Sc. Thesis, Al-Fatah University, Libya, spring 1996.
- [6] Barony, S., Galuta, E., Tuhami, A., Analysis of Cylindrical Shells Using Mixed Formulation of Curved Finite Strip Element, International Journal of Innovative Science, Engineering & Technology, Vol. 4 Issue 5, May 2017.
- [7] Barony S. Y and Tottenham H., The analysis of rotational shells using curved ring elements and mixed variational formulation, Int. J. Num. Meth. Eng., vol. 10, 1976, pp. 861-872.
- [8] Tuhami A., Analysis of Cylindrical Shells Using Mixed Formulation of Curved Finite Strip Element, M. Sc. Thesis, University of Tripoli, 2007.
- [9] Al-Salah W., Mixed Curved Finite Strip Analysis of Cylindrical Shells Using Spline Function, M. Sc. Thesis, University of Tripoli, 2010.
- [10] Scordelis, A. and Lo, K., Computer Analysis of Cylindrical Shells, J. Am. Conc., Inst., 61, No. 5, May 1964.